View metadata, citation and similar papers at core.ac.uk

brought to you by CORE

provided by Northumbria Research Link

Northumbria Research Link

Citation: Yurduseven, Okan, Smith, Dave, Pearsall, Nicola, Forbes, Ian and Johnston, David (2012) A transparent multiband solar patch array antenna. In: Loughborough Antennas and Propagation Conference (LAPC2012), 12-13 November 2012, Loughborough University.

Published by: UNSPECIFIED

URL: http://www.lapconf.co.uk/

This version was downloaded from Northumbria Research Link: http://nrl.northumbria.ac.uk/10153/

Northumbria University has developed Northumbria Research Link (NRL) to enable users to access the University's research output. Copyright © and moral rights for items on NRL are retained by the individual author(s) and/or other copyright owners. Single copies of full items can be reproduced, displayed or performed, and given to third parties in any format or medium for personal research or study, educational, or not-for-profit purposes without prior permission or charge, provided the authors, title and full bibliographic details are given, as well as a hyperlink and/or URL to the original metadata page. The content must not be changed in any way. Full items must not be sold commercially in any format or medium without formal permission of the copyright holder. The full policy is available online: http://nrl.northumbria.ac.uk/policies.html

This document may differ from the final, published version of the research and has been made available online in accordance with publisher policies. To read and/or cite from the published version of the research, please visit the publisher's website (a subscription may be required.)

www.northumbria.ac.uk/nrl

northumbria UNIVERSITY

University Library

A Meshed Multiband Solar Patch Array Antenna

Okan Yurduseven, David Smith, Nicola Pearsall, Ian Forbes and David Johnston
School of Computing, Engineering and Information Sciences
Northumbria University
Newcastle upon Tyne, NE1 8ST, United Kingdom
okan.yurduseven@northumbria.ac.uk

Abstract—**In this paper, a meshed multiband solar patch array antenna, consisting of a polycrystalline silicon solar panel working as a ground plane whilst generating a DC power output of 1.48 W as a result of the photovoltaic effect with a measured solar efficiency of 14.95%, is proposed for GSM 900/1800/1900, UMTS 1900, 3.5 GHz band WiMAX and C-band applications. The proposed solar patch array antenna introduces a further potential of solar cells to be effectively used as embedded elements within communication systems, raising the awareness of solar energy and offering a practical solution to the requirement for the incorporation of solar cells/panels with microwave antennas within solar powered autonomous communication systems suffering from increasing dimensions due to the separate involvement of solar panels and microwave antennas.**

Keywords-solar patch array antenna; meshed patch antenna; solar energy; polycrystalline silicon solar cell

I. INTRODUCTION

The concept of solar powered communication systems has attracted much attention due to its potential of meeting the requirement of powering these systems without the need of an electric grid connection, which is a significant factor to be considered when it comes to powering communication systems in places where there is no available grid connection, such as space or the isolated regions on Earth. Besides, as a sustainable energy source, the concept of using the Sun to generate electricity has a potential of addressing the threat of global warming, which is caused by the increasing level of CO_2, a gas which allows the visible light radiated by the Sun to pass through the atmosphere whilst trapping the infrared radiation re-radiated back from the ground resulting in heating up the Earth, released as a result of the use of fossil fuels.

As a sustainable carbon-free alternative to fossil fuels, solar energy has become a primary choice to power communication systems in an environmental-friendly way [1-3]. A significant problem that is brought by the standalone introduction of solar panels and microwave antennas within solar powered autonomous communication systems is the ineffective use of the limited space available for low-profile systems.

An increasing amount of research has recently been conducted in order to provide low-profile compact solar antenna designs capable of generating DC power output whilst receiving and transmitting RF/microwave signals. Recent work has demonstrated a transparent microstrip patch antenna, which is made out of an expensive conductive transparent film, AgHT-4, with a minimum visible light transmission of 75% [4]. The proposed antenna resonates at a single frequency band with an impedance bandwidth of 4.3%, limiting the usability of the antenna in multiband/wideband communication systems. A planar antenna design comprising printed slot fed GaAs solar cells working as radiating elements, replacing conventional metal patches, has been demonstrated [5]. Whereas the return loss (S_{11}) and gain measurements have been taken and reported as 8% and 4.22 dBi across the frequency band of 2.753-2.983 GHz, it is not known how efficient the proposed solar antenna is from the solar point of view as the DC solar performance measurements have not been performed. The integration of a polycrystalline silicon solar cell with a solid non-transparent microstrip radiating patch element has been proposed [6], in which the patch is placed above, shadowing the cell and resulting in non-uniformity in the illumination intensity across the cell surface and so reducing the total solar efficiency. The proposed antenna offers an impedance bandwidth of 3.11%, operating at the centre frequency of 2.19 GHz. The proposals of a solar monopole for low-power transceivers and a dipole antenna combined with polycrystalline silicon solar cells have also been made [7, 8].

This work proposes a meshed multiband solar patch array antenna resonating at multiple frequency bands required for GSM 900/1800/1900, UMTS 1900, 3.5 GHz band WiMAX and C-band applications. The proposed solar patch array antenna consists of an array of 2 meshed transparent radiating patch elements, effectively combined with a polycrystalline silicon solar panel working as a ground plane. Whilst the S_{11} and far-field E-plane and H-plane radiation pattern measurements have been taken by using a network analyser in an anechoic chamber, the DC solar performance measurements of the fabricated solar antenna have been performed in a solar chamber containing metal halide lamps with a colour temperature of 5200K, providing a uniform illumination intensity of 1000 W/m^2 upon the proposed solar antenna within the chamber equivalent to the intensity used for the Standard Test Conditions for testing photovoltaic cells.

II. DESIGN AND FABRICATION OF THE TRANSPARENT SOLAR ARRAY ANTENNA

The fabricated meshed solar patch array antenna is shown in Fig. 1.

978-1-4673-2220-1/12/$31.00 ©2012 IEEE

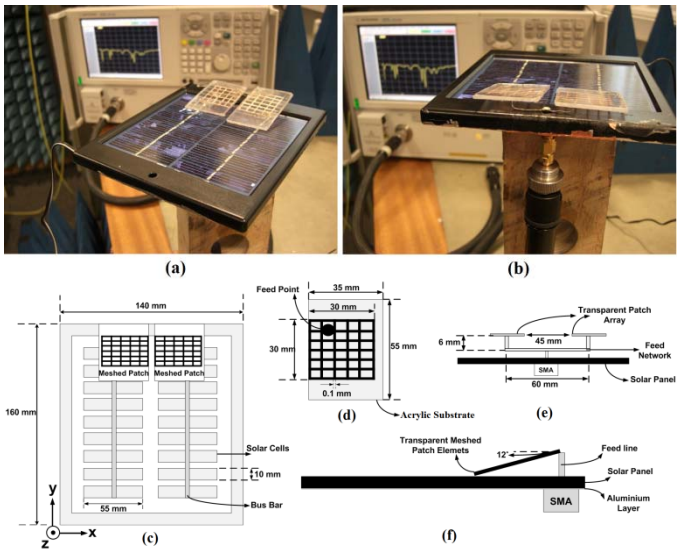

Figure 1. Fabricated meshed solar patch array antenna (a) front-view (b) back-view (c) top view-dimensions (d) meshed patch element (e) back view-feed network (f) side view-tilted patch configuration.

As can be seen in Fig. 1*c*, the proposed meshed solar patch array antenna consists of an array of 2 meshed copper patch elements printed on 2 mm thick transparent acrylic substrates with a dielectric constant of 3.6 and a loss tangent of 0.015. Fig. 1*d* provides a closer look at the structure of a single radiating meshed patch element within the proposed array configuration. The transparency of each meshed patch element within the array has been calculated as 95%, which is sufficient enough for sunlight incident upon the solar panel to pass through the array without being blocked or reflected significantly. In order to minimise the coupling between the radiating meshed patch elements within the array, the separation distance has been set to 45mm, which is larger than the quarter wavelength at the centre resonance frequency of 1.92 GHz, 39.06mm.

Investigation into the effects of meshing conventional solid copper microstrip patch elements has been carried out [9], and it has been demonstrated that meshing the radiating patch element itself does not have a significant effect on the radiation characteristics of microstrip patch antennas.

The meshed patch array has been fed through a split line feed as can be seen in Fig. 1*e*. The feed network consists of a single vertical line with a length of 10mm, connected to the core conductor of the coaxial feed cable through an SMA connector, breaking up into 2 vertical lines with a length of 6 mm separated by a distance of 60 mm; each has been connected to the feed points of the meshed patches as a probe feed element as illustrated in Fig. 1*d* and Fig. 1*e*.

Below the radiating meshed patch elements a polycrystalline silicon solar panel has been introduced to be used as a ground plane element within the proposed solar antenna design as illustrated in Fig. 1*f*. The solar panel consists of 18 series connected polycrystalline silicon solar cells; each has dimensions of 55x10 mm as can be seen in Fig. 1*c*.

As is illustrated in Fig. 1*f*, a tilt angle of 12˚ has been introduced in the suspended geometry of the meshed patch array antenna in the y-z plane, resulting in an enhancement in the multiband return loss performance of the proposed solar antenna compared to the conventional flat suspension.

The optimization of the tilt angle has been carried out by using a generic algorithm in CST Microwave Studio, through which an angle sweep between 0˚ (the flat position) and 20˚ has been performed. Considering the initial sweep step angle of 0.5˚ selected at the beginning of the optimization process in order to increase the accuracy and the precision of the optimal solution, the required total simulation time to perform the sweeping between these angles would be significant unless any other supporting techniques were used. The use of a generic algorithm, which has enabled the optimal tilt angles, at which superior multiband characteristics are obtained, to be selected for the next iterations to evolve towards better solutions whilst the rest non-optimal ones are eliminated at each iteration, has resulted in a considerable decrease in the total required simulation time. The optimum multiband S_{11} characteristics have been obtained at the tilt angle of 12˚.

The polycrystalline solar panel is encapsulated between the acrylic on the top and an FR4 dielectric layer at the bottom. The encapsulation of the panel allows large-scale arrays of the proposed solar array antenna to be designed for long-range solar powered communication systems, such as satellites, for which superior antenna gain characteristics and DC solar performance are required. Each polycrystalline silicon solar cell within the panel consists of 2 metal DC contacts, the solid bottom and the grid top, with silicon sandwiched between these contacts, comprising an n-doped layer on the top and a p-doped layer at the bottom, as illustrated in Fig. 2.

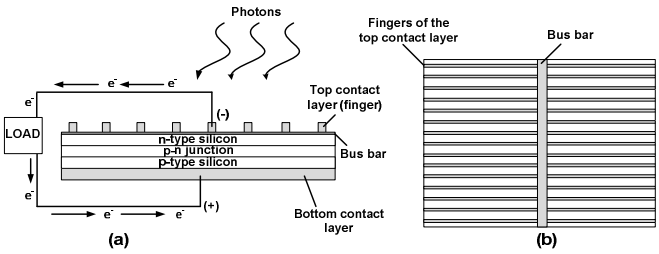

Figure 2. Structure of the polycrystalline silicon solar cell.

Due to the existence of the homogenous solid aluminum DC contact layer at the bottom as depicted in Fig. 2, solar cells can be used as radiating or ground plane elements within planar antenna systems [10].

Consideration should be given when it comes to the use of panel designs, as whilst the panels consisting of parallel connected solar cells have a homogeneous metal plate underneath, connecting the bottom DC contacts of individual solar cells together, the same does not apply to the panels consisting of series connected cells, in which the bottom DC contacts and the top grid layers are connected one to another within the panel.

As the polycrystalline solar cells within the panel used in this work are connected in series, providing a high DC voltage output, it is not possible to use the panel as a homogeneous metal plate working as a solid ground plane element without performing any modifications in the geometry of the solar

panel. The modification has been made by using a thin aluminum layer covering underneath the dielectric layer at the bottom of the panel. It should also be reported here that this process does not have any effects on the DC solar performance of the panel.

A significant factor considered in this work is the effect of the suspended transparent radiating patch elements, placed above the solar panel, on the DC solar performance of the proposed solar antenna. Although the transparency of both meshed patch elements has been calculated as 95%, providing a sufficient transparency in order for the radiating patches not to block the sunlight incident upon the solar panel significantly, the existence of the transparent patch elements results in a non-uniform illumination intensity across the surface of the panel, which has a potential of becoming a major problem when it comes to the total DC output current level generated by the solar panel as the total current output is limited by the current of each polycrystalline silicon solar cell within the panel. A significant decrease in the DC current output level of a single solar cell would also reduce the total DC current output level of the panel dramatically.

The reason behind the selection of the acrylic as a substrate material and the use of meshing technique on the copper patch elements printed on the acrylic substrates is to minimise the non-uniformity by increasing the transparency to avoid such a dramatic decrease in the total DC current output level that can be withdrawn from the proposed solar antenna.

III. Measurement Results and Discussion

A. Antenna Measurements

The simulated and measured S_{11} patterns of the fabricated meshed solar patch array antenna taken across the frequency band of 900 MHz - 6 GHz are shown in Fig. 3.

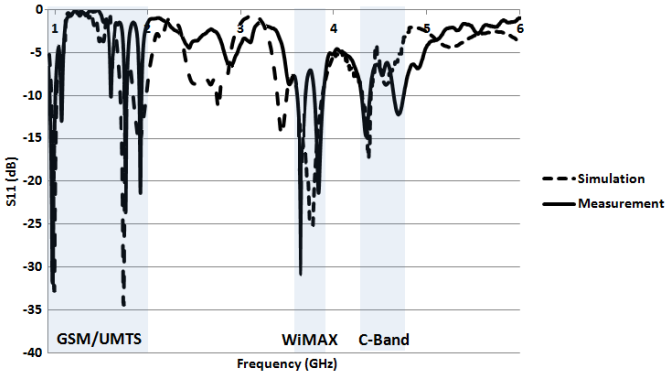

Figure 3. Simulated and measured S_{11} patterns.

As can be seen in Fig. 3, there is good agreement between the simulation and the measurement results. The proposed solar antenna resonates at multiple frequency bands, covering GSM 900/1800/1900, UMTS 1900, 3.5 GHz WiMAX and C-band applications.

The E-plane and H-plane far-field radiation pattern measurements of the fabricated meshed solar patch array antenna have been taken in an anechoic chamber with an input power level of 14 dBm. A circularly polarised conical spiral antenna with a constant gain of 4 dBi over the frequency band of 1-10 GHz has been used as a reference antenna in order to determine the gain values of the fabricated meshed solar patch array antenna.

The measured maximum E-plane and H-plane gain readings of the proposed solar antenna have been taken at the resonance frequencies of 0.9, 1, 1.08, 1.61, 1.76, 1.92, 3.64, 3.83, 4.3 and 4.7 GHz, and are given in Table I.

TABLE I. Measured E-Plane and H-Plane Gain Values Across Multiple Resonance Frequency Bands

Frequency (GHz)	Gain (dBi)	
	E-Plane (y-z)	*H-Plane (x-z)*
0.9	3	2.1
1	3.5	2.5
1.08	2	0.6
1.61	5.2	2.3
1.76	4.8	3.2
1.92	5.1	4.3
3.64	9.4	3.3
3.83	9.5	6.2
4.33	6.1	2
4.7	5.8	4.5

The gain values in Table I are the total measured gain values, which take all the losses into account, including the losses that are introduced by the existence of the lossy silicon layer within the structure of polycrystalline silicon solar cells that together form the panel and ohmic losses.

The obtained far-field radiation patterns across the operating frequencies are shown in Fig. 4. In order to increase the readability, both E-plane and H-plane far-field radiation patterns have been broken up into 2 graphs; the first graphs illustrate the patterns taken at the frequencies of GSM/UMTS bands whilst the second graphs are for the WiMAX and C-band networks. All E-plane and H-plane far-field radiation patterns have been normalised to maximum E-Plane and H-plane gain values of 9.5 dBi and 6.2 dBi respectively, which have been obtained at 3.83 GHz as can be seen in Table I.

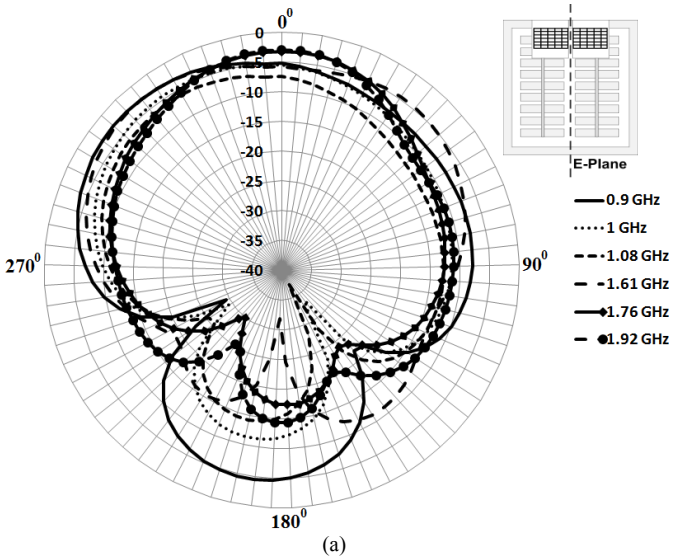

(a)

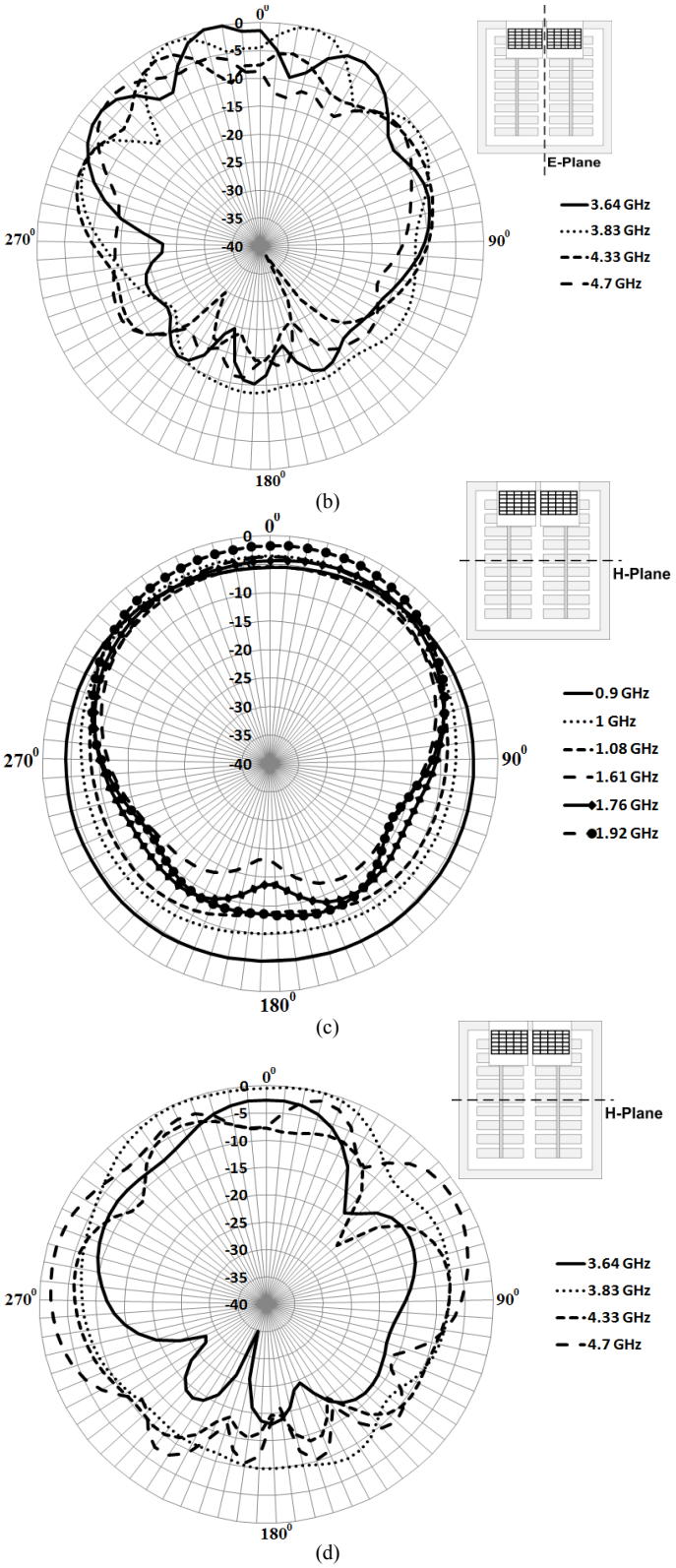

Figure 4. Measured E-plane (normalized to maximum gain of 9.5 dBi) and H-plane (normalized to maximum gain of 6.2 dBi) far-field radiation patterns (a) E-Plane for GSM/UMTS bands (b) E-Plane for WiMAX and C-band (c) H-plane for GSM/UMTS bands (d) H-plane for WiMAX and C-band.

B. Solar Measurements

The solar measurements of the proposed solar antenna have been taken in a solar chamber containing metal halide lamps with a colour temperature of 5200K, providing a uniform illumination intensity of 1000 W/m^2 fulfilling the requirements for the Standard Test Conditions for testing photovoltaic cells. The solar chamber and the measurement setup within the chamber are illustrated in Fig. 5.

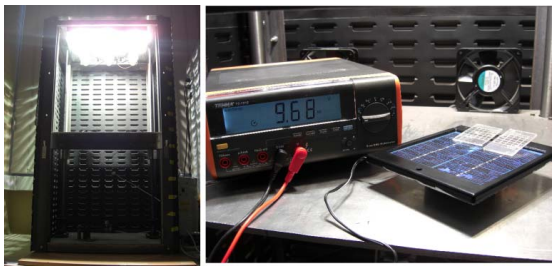

(a) (b)

Figure 5. DC solar measurement (a) solar chamber (b) measurement setup within the chamber.

In this paper, meshing the radiating elements and printing them on transparent acrylic substrates is offered as a solution to minimise the shadowing and to decrease the non-uniformity in the illumination intensity over the solar panel compared to the conventional use of non-transparent solid copper patch elements printed on non-transparent dielectric substrates, such as FR4. In order to demonstrate the efficiency of the proposed transparent configuration by determining the effect of the transparent radiating patch array element on the DC solar performance of the fabricated solar antenna, solar measurements have been taken in the solar chamber without any radiating elements placed above the solar panel followed by the measurements taken with the transparent and non-transparent radiating patch elements placed above. It should be noted here that the non-transparent solid patch array consists of an array of 2 conventional solid copper patch elements printed on non-transparent FR4 dielectric substrates.

A series of resistors, from 10Ω to 2.7kΩ, have been connected to the terminals of the solar panel as a load and the voltage and current readings have been taken for each configuration. The I/V curves have been obtained and the solar efficiencies have been calculated for each design mentioned above.

In Fig. 6, the obtained I/V curves are illustrated.

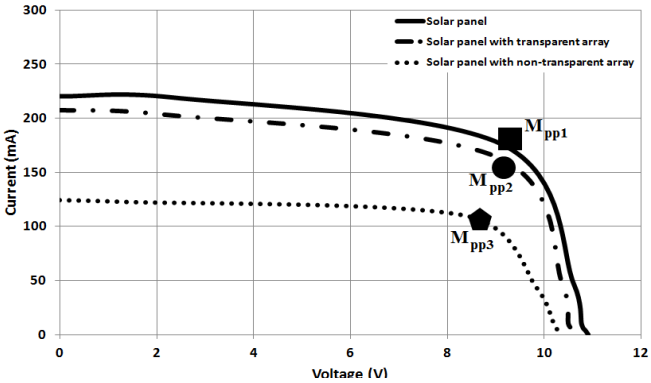

Figure 6. Measured solar I/V curves.

The solar panel without any elements placed above generates a measured open circuit voltage of 10.9 V with a short circuit current of 220.3 mA. At the maximum power point of the solar panel without any radiating elements placed above, M_{pp1} in Fig. 6, where the DC power output is maximum, the measured voltage and current readings have been recorded as 9.1 V and 176.4 mA, that together provides a maximum DC power output of 1.6 W. When the proposed transparent radiating patch array is placed above the solar panel, the open circuit voltage drops by 2.84%, from 10.9 V to 10.59 V, whilst the short circuit current decreases by 5.85%, from 220.3 mA to 207.4 mA. At the maximum power point, M_{pp2}, the measured voltage and current values have been recorded as 9 V and 164.5 mA respectively, equivalent to a maximum DC power output of 1.48 W. The use of the non-transparent solid patch array, in the same dimensions with the transparent one, on the other hand, degrades the solar performance significantly by resulting in a sharp decrease of 43.6% in the measured short circuit current, from 220.3 mA to 124.3 mA, with a drop of 4.86% in the open-circuit voltage, from 10.9 V to 10.37 V. At the maximum power point, M_{pp3}, the measured voltage and current values have been observed as 8.41 V and 109.7 mA, providing a maximum DC power output of 0.92 W.

Table II summarises the DC solar performance readings taken for the solar panel combined with the proposed transparent radiating patch array and the non-transparent element respectively.

TABLE II. MEASURED DC SOLAR PERFORMANCE CHARACTERISTICS

Configuration	V_{OC} (V)	I_{SC} (mA)	V_{max} (V)	I_{max} (mA)	P_{max} (W)	η (%)
Panel	10.9	220.3	9.1	176.4	1.6	16.2
Panel tr. array	10.59	207.4	9	164.5	1.48	14.95
Panel non tr. array	10.37	124.3	8.41	109.7	0.92	9.31

Considering the illumination intensity of 1000 W/m^2 within the chamber, and the total surface area of the panel formed by 18 series connected polycrystalline silicon cells, each 5.5 cm^2 providing a total area of 99 cm^2 altogether, the total incident power can be calculated as 9.9 W, which then can be used to determine the efficiency of the mentioned configurations above.

The equation that has been used to calculate the solar efficiency can be given as follows:

$$\eta = \frac{Mpp}{Pi.A} \quad (1)$$

In (1), M_{pp} represents the total DC power output that can be obtained from the panel at the maximum power point on the I/V curve whilst P_i and A are for the illumination intensity of the solar chamber over the solar surface and the total solar surface area of the panel respectively.

Whilst the solar efficiency of the solar panel itself has been calculated as 16.2%, the introduction of the radiating transparent patch array element has resulted in a slight decrease of 1.25% in the solar efficiency, which has been recorded as 14.95%. The non-transparent solid patch array element, on the other hand, has decreased the solar efficiency by 6.89%, from 16.2% to 9.31%.

IV. CONCLUSION

In this work, a meshed multiband solar patch array antenna is demonstrated for GSM 900/1800/1900, UMTS 1900, 3.5 GHz band WiMAX and C-band applications. The proposed transparent solar antenna generates a DC power output of 1.48 W as a result of the photovoltaic effect. The measured S_{11} and far-field radiation pattern results show the suitability of the proposed solar antenna for multiband communication networks whilst the DC solar measurements with promising results prove how feasible it is to combine solar cells/panels with microwave antennas into multifunctional low-profile compact devices compared to the solar powered autonomous communications systems in which these elements are incorporated separately resulting in a compromise in the utilization of the limited available space.

REFERENCES

[1] R. Prasad and R. Mehrotra, "A solar powered telecom architecture for off-grid locations", Technical Symposium at ITU Telecom World, pp. 205-210, October 2011.

[2] T. K. Das, A. K. Das, and A. Das, "Solar Power of Mobile Transmitter/Receiver Tower Antennas in Remote Areas", 2nd Asian Himalayas International Conference on Internet, pp. 1-4, November 2011.

[3] B. Gaudette, V. Hanumaiah, S. Vrudhula, and M. Krunz, "Optimal range assignment in solar powered active wireless sensor networks", IEEE INFOCOM, pp. 2354-2362, March 2012.

[4] M. J. R. Ons, S. V. Shynu, M. J. Ammann, S. J. McCormack, and B. Norton, "Transparent patch antenna on a-Si thin film glass solar module", Electronics Letters, vol. 47, pp. 85-86, January 2011.

[5] S. Vaccaro, J. R. Mosig, and P. De Maagt, "Making planar antennas out of solar cells", Electronics Letters, vol. 38, pp. 945-947, August 2002.

[6] S. V. Shynu, M. J. R. Ons, P. McEvoy, M. J. Ammann, S. J. McCormack and B. Norton, "Integration of microstrip patch antenna with polycrystalline silicon solar cell", IEEE Transactions on Antennas and Propagation, vol. 57, pp. 3969-3972, December 2009.

[7] M. Danesh, J. R. Long, and M. Simeoni, "Small-area solar antenna for low-power UWB transceivers", 4th European Conference on Antennas and Propagation, pp. 1-4, April 2010.

[8] S. V. Shynu, M. J. R. Ons, G. Ruvio, M. J. Ammann, S. McCormack, and B. Norton, "A microstrip printed dipole solar antenna using polycrystalline silicon solar cells", IEEE Antennas and Propagation Society International Symposium, pp. 1-4, July 2008.

[9] G. Clasen and R. Langley, "Meshed patch antennas", IEEE Transactions on Antennas and Propagation, vol. 52, pp. 1412-1416, June 2004.

[10] N. Henze, A. Giere, H. Fruchting, and P. Hoffman, "GPS patch antenna with photovoltaic solar cells for vehicular applications", IEEE 58th Vehicular Technology Conference, vol. 1, pp. 50-54, Oct. 2003.